On the radial pellet cloud drift in stellarator plasmas

G. Kocsis[1], J. Baldzuhn[2], C. Biedermann[2], R. Bussiahn[2], A. Buzás[1], G. Cseh[1], I. García-Cortés[3], M. Krause[2], K.J. McCarthy[3], D. Medina-Roque[3], N. Panadero[3], T. Szepesi[1], N. Tamura[4,5], Th. Wegner[2], TJ-II Team[3] and W7-X Team[*]

[1] *Centre for Energy Research, Budapest, Hungary*
[2] *Max-Planck-Institute for Plasma Physics, Greifswald, Germany*
[3] *Laboratorio Nacional de Fusion, CIEMAT, Madrid, Spain*
[4] *National Institute for Fusion Science, National Institutes of Natural Sciences, Toki, Japan*
[5] *The Graduate University for Advanced Studies, SOKENDAI, Toki, Japan*
[*] *See author list of Thomas Sunn Pedersen et al 2022 Nucl. Fusion 62 042022*

The cryogenic pellet fuelling efficiency is - among others - largely determined by the drift properties of the high-pressure pellet cloud elongated along the magnetic field line crossing the pellet ablating in the hot plasma. In tokamaks, the pellet cloud drift created by the gradient of the axially symmetric magnetic field - which pushes the pellet cloud to the low field side (LFS) of the plasma - clearly enhances the fuelling efficiency of pellets injected from the inboard side of the torus [1].

In the much more complex (non-axially symmetric) magnetic field of stellarators the advantage of the inboard side pellet injection does not necessarily apply [2]. Most probably because the direction of grad-B in a poloidal plane looks more complicated than in a tokamak, and it does vary with the toroidal angle, it can even reverse along the high-pressure, field line elongated pellet cloud.

To better understand the radial drift of the pellet cloud in the stellarator geometry, experiments were performed in the W7-X and TJ-II stellarators. Both cryogenic (Hydrogen) and tracer-encapsulated solid (TESPEL) pellets were injected into the plasma and the evolution of the radiation distribution of the pellet cloud particles was measured by spectroscopic methods using fast framing cameras viewing from different directions. Wavelength selection by interference filters was used to separate certain ionic species of the cryogenic H pellet (Hα and Bremsstrahlung) and polystyrene polymer $(C_8H_8)_n$ shell of the TESPEL (C I, C II, C III). The temporal resolution of the fast camera observation is up to 700 kHz, which allows us to resolve the detachment and the radial drift of the pellet cloud.

Fast framing movies about Hydrogen pellets injected into the W7-X (cylindrical with 2mm size, speed up to 250m/s, mass reduced: HFS (inboard) by 0.6, LFS (outboard) by 0.25 [2]) and TJ-II (diameter: 0.42-0.76mm, speed: 600-1200m/s [3]) stellarators clearly show the drifting clouds both with Hα and Bremsstrahlung filters (see Fig. 1. and Fig. 2). The observed drift frequency (cloud detachment frequency) was around 100kHz (W7-X) and higher (TJ-II). The speed of the drifting cloud was found in the order of 5000m/s. Obvious outward radial drift was observed for the cases injected from the outboard (LFS) of both stellarators. The inboard (HFS) injection in W7-X is less clear but seems to be outward drift. This is also supported by the fact, that the pellet is decelerated during the ablation which is the consequence of the asymmetric cloud shielding caused by the outward directed cloud drift. There was a hint that when the pellet is at a large magnetic island (TJ-II, 3/2 at rho=0.35) drift activity is suppressed. The explanation might be the limited heat flux at this rational surface, but this observation has yet to be further investigated in dedicated experiments.

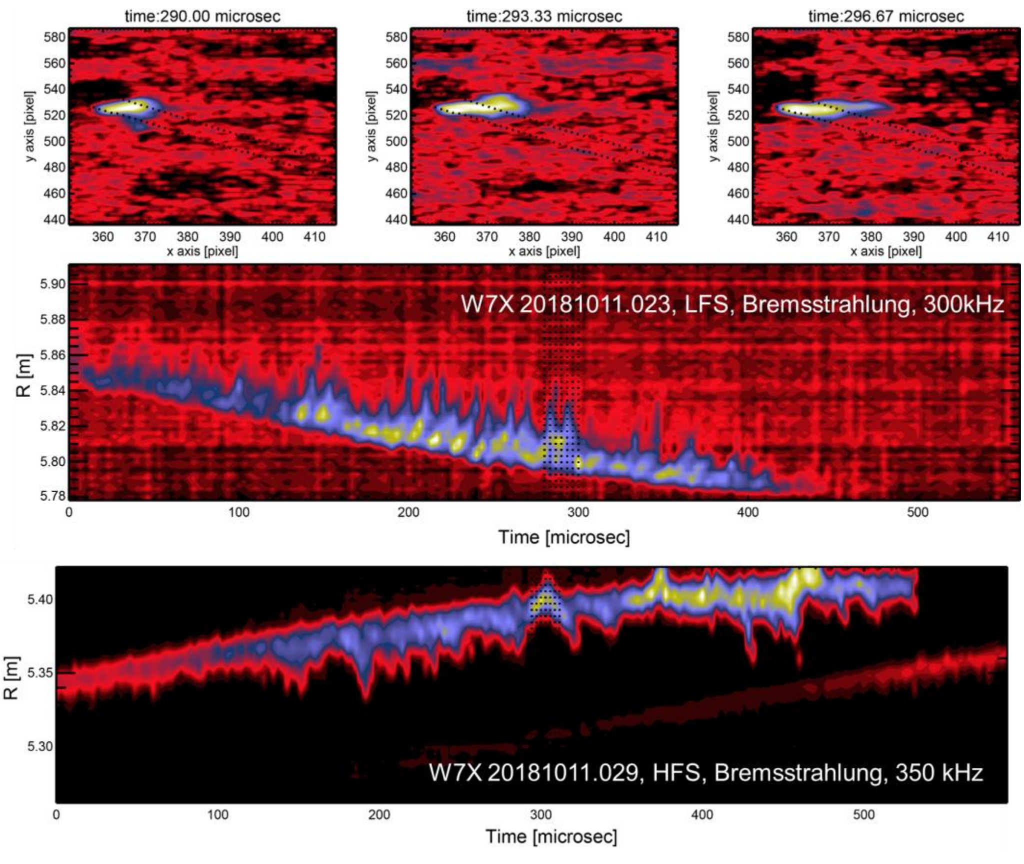

Fig. 1. Hydrogen pellet injection into W7-X. The upper figures are consecutive snapshots of the LFS injection (20181011.023) made by Bremsstrahlung filter using a tangential view (AEQ41 port). Pellet flies from right to left, the detached, drifting cloud moves outwards (to the right). Pellets are tracked and the frames are cut along the pellet trajectory and this radiation cuts (vertical axis, major radius along the pellet trajectory) are plotted as a function of time (horizontal axis for LFS (middle plot., 20231011.023) and HFS (lower plot, 20181011.029). Both cases show clear pellet deceleration during ablation and outward drift.

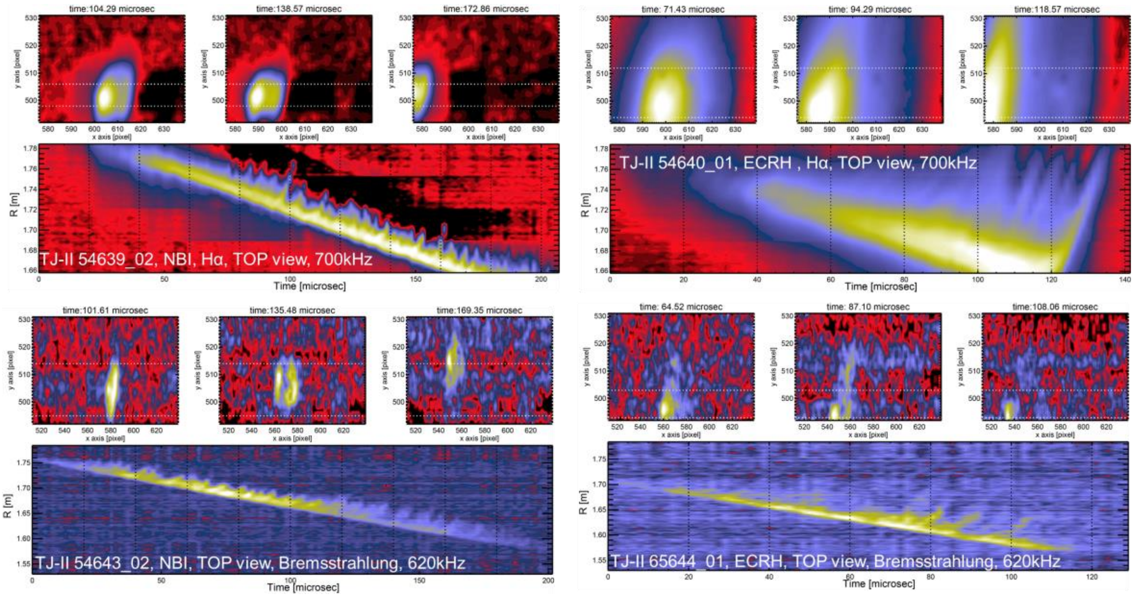

Fig. 2. Hydrogen pellet injection into TJ-II plasmas both with ECRH (right plots, Te ~ 1keV, #54640 and #65644) and NBI (left plots, Te ~ 0.5keV, #54639 and #54643) heating. TOP view is used upper figures are with Hα the lower ones with Bremsstrahlung filters. As at Fig. 1. snapshots at selected times and the radiation along the pellet trajectory as a function of time are plotted for the above four cases. The distribution of the Hα radiation is much wider for the ECRH heating case with higher electron temperature. The outward drift is clearly visible for all cases.

TESPEL ablation and cloud drift was investigated on both stellarators [4],[5], but our study concentrated only on the polystyrene polymer $(C_8H_8)_n$ shell particles, namely C I, C II, C III. C III radiation well characterizes the ionized, field line elongated pellet cloud, i.e. its drift, while C I is concentrated around the TESPEL. Snapshots (see Fig. 3.) about C III radiation of the TESPEL cloud shows a two-peak structure along the magnetic field line. The pellet is probably at the centre of cloud as seen on images recorded with C II filter (Fig. 4.). Probably because of the lower energy flux exposing the pellet and its cloud the C III radiation distribution looks different in TJ-II plasmas: C III radiation is close to the TESPEL initially, it appears in the drifting cloud only after the cloud is separated/detached from the pellet (see Fig. 5). The cloud drift is clearly visible on C III images for both stellarators. The frequency of the drift event – similarly to the Hydrogen pellet injection experiments - is in the order of 100kHz for W7-X and higher for TJ-II. The speed of the pellet cloud drift is larger than 5000m/s for both stellarators.

Acknowledgement: This work has been carried out within the framework of the EUROfusion Consortium, funded by the European Union via the Euratom Research and Training Programme (Grant Agreement No 101052200 - EUROfusion). Views and opinions expressed are however those of the author(s) only and do not necessarily reflect those of the European Union or the European Commission. Neither the European Union nor the European Commission can be held responsible for them.

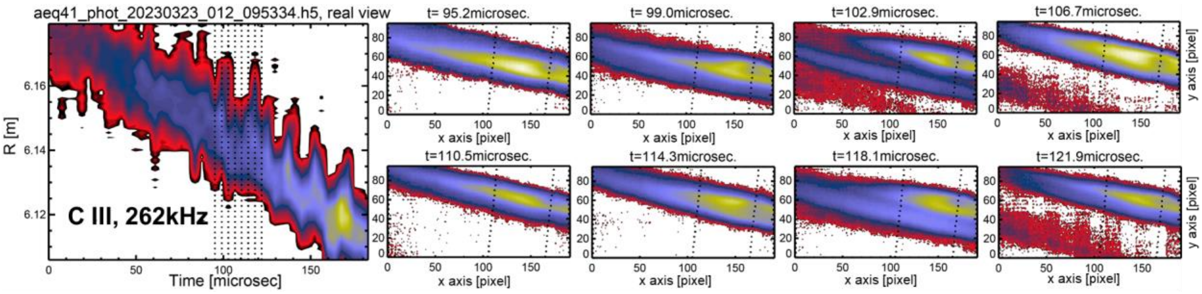

Fig. 3. TESPEL injection into W7-X (20230323.012): consecutive snapshots (right figures) and the history of the radiation along the TESPEL trajectory (left) recorded with C III filter using the AEF41 view (from below).

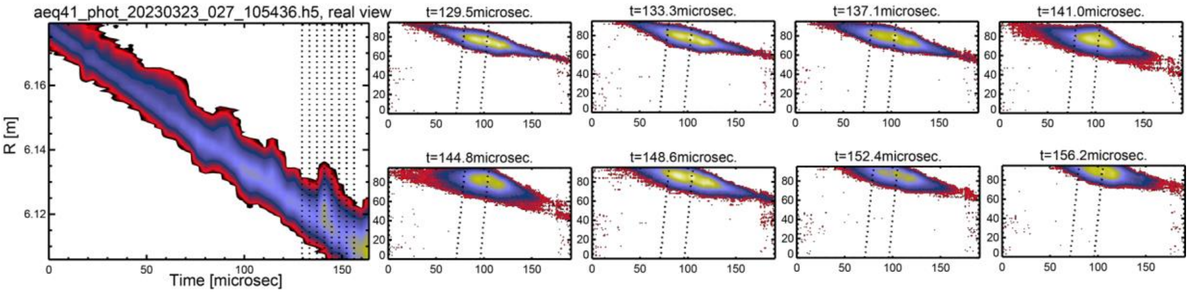

Fig. 4. TESPEL injection into W7-X (20230323.027): consecutive snapshots (right figures) and the history of the radiation along the TESPEL trajectory (left) recorded with C II filter using the AEF41 view (from below).

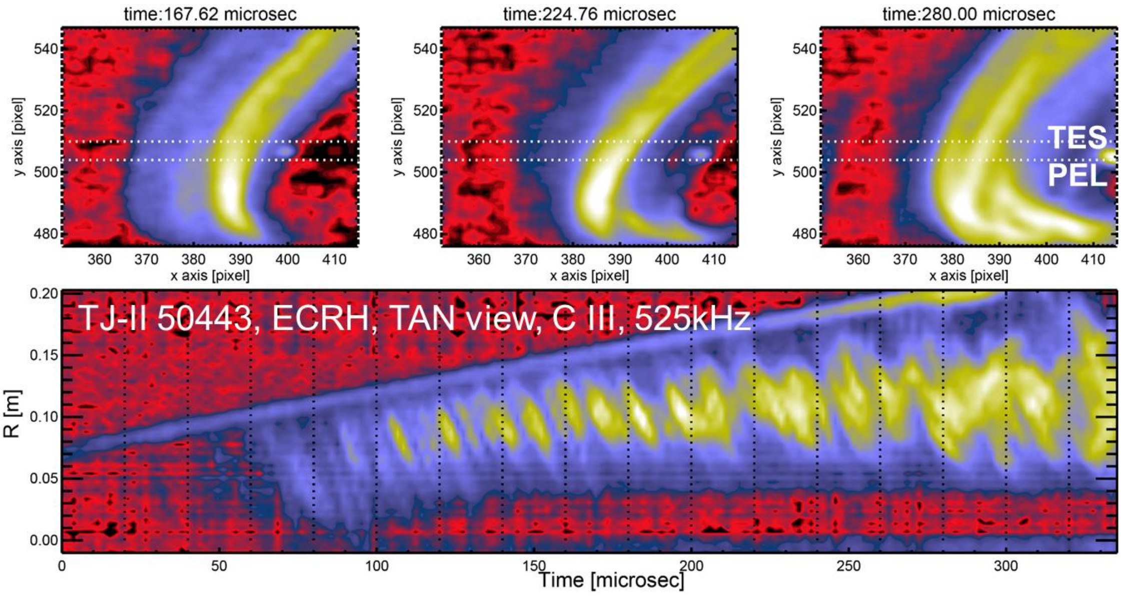

Fig. 5. TESPEL injection into TJ-II (#50443): selected snapshots (upper figures, pellet flies from left to right) and the history of the C III radiation along the TESPEL trajectory (lower plot) recorded using a tangential view.

References:

[1] P.T. Lang et al 1997 Phys. Rev. Lett. 79 1487
[2] J. Baldzuhn et al 2019 Plasma Phys. Control. Fusion 61 095012
[3] N. Panadero et al 2018 Nucl. Fusion 58 026025
[4] R. Bussiahn et al 2018 Rev. Sci. Instrum. 89 10K112
[5] N. Tamura et al 2016 Rev. Sci. Instrum. 87 11D619.